

Effect of Support on Hydrogenolysis of Glycerol over Cu Catalysts

^{1,2}JIE ZHOU, ^{1,2}SHUNLI HAO*, ¹NING ZHAO, ¹FUKUI XIAO, ¹WEI WEI AND ^{1,3}YUHAN SUN

¹State Key Laboratory of Coal conversion, Institute of Coal Chemistry,
Chinese Academy of Sciences, Taiyuan, 030001, P.R. China.

²Graduate School of the Chinese Academy of Sciences, Beijing, 100049, P.R. China.

³Low Carbon Energy Conversion Center, Shanghai Advanced Research Institute,
Chinese Academy of Sciences, Shanghai, 201203, P.R. China.

haosl@sxicc.ac.cn*

(Received on 12th September 2011, accepted in revised form 9th March 2012)

Summary: Hydrogenolysis of biomass-derived glycerol is an alternative route to produce 1, 2-propanediol. Supported Cu catalysts were prepared by the wetness impregnation method and characterized by N₂ adsorption-desorption, X-ray powder diffraction (XRD), X-ray photoelectron spectroscopy (XPS), Fourier transformed infrared spectroscopy (FT-IR), temperature programmed desorption of NH₃ (NH₃-TPD) and temperature programmed reduction (TPR) techniques, and then tested for glycerol hydrogenolysis. It was found that the nature of support significantly affected the performance of the catalysts, revealing a correlation between catalytic activity and total acidity. Compared with ZrO₂, SiO₂ and HZSM-5, γ -Al₂O₃ showed superior performance due to its surface properties, and with 20wt% Cu loaded, glycerol conversion and 1, 2-propanediol selectivity reached 85.05% and 85.71% at 513 K and 6 MPa H₂, respectively.

Keywords: Glycerol; Hydrogenolysis; 1, 2-Propanediol; Support; Acidity.

Introduction

Biomass has received much attention being a new energy source because of its renewable and carbon-neutral. Especially, biodiesel [1] has been proved to be a potential environmentally friendly diesel fuel substitute or extender. With the increase of annual world production of biodiesel, the crude glycerol, as the by-product, will increase to over 400 million liters per year and then the market will likely to be saturated due to the limited demand for glycerol in medicines, cosmetics, and sweetening agents. Recently, attention has been paid to the conversion of glycerol to high value-added products, such as propylene glycol [2-4], acrolein [5-8] and hydrogen [9-12]. Thus, glycerol is regarded as one of the building blocks in the bio-refinery feedstock.

1, 2-propanediol (1, 2-PD), one of the products in the hydrogenolysis of glycerol, could be used as a raw material of polyester resins, food products, antifreeze, liquid detergents, pharmaceuticals, etc. At present, the manufacture of 1, 2-PD is mainly based on the hydration of propylene oxide derived from petroleum. So, glycerol hydrogenolysis to 1, 2-PD represents a sustainable process with valuable potential applications [2-4, 13].

Currently, the hydrogenolysis of glycerol to 1, 2-PD has been reported in either gaseous or liquid

phases reaction process, involving various catalysts, such as the supported Rh [3, 13, 14], Ni [15], Ru [14, 17-26], Pt [20, 27, 28], and Cu [13, 16, 26, 29-39]. The previous results demonstrated that noble metal catalysts were usually more active than Cu based catalysts towards the hydrogenolysis reaction, yet with low selectivity to 1,2-PD. It has also been reported that bi-functional catalysis played a vital role in the hydrogenolysis of the glycerol reaction [3, 13, 16, 18, 33, 37], including the dehydration glycerol on acid sites, and then the hydrogenation of the intermediate on metal sites.

To keep those in mind, the hydrogenolysis of glycerol was investigated to understand the role of support in the present work. The support materials such as γ -Al₂O₃, ZrO₂, SiO₂ and HZSM-5 were used. In addition, the reaction was also carried out at different reaction conditions to optimize the selective formation of 1, 2-PD.

Results and discussion

Texture and Phase Structure

N₂ adsorption-desorption was employed to determine the textural properties of the supported Cu catalysts (BET surface area, average pore diameter

*To whom all correspondence should be addressed.

and pore volume, Table-1). The introduction of copper caused a slight decrease in the specific surface area of samples compared to the supports, especially for the catalyst Cu/SiO₂. These phenomena could be probably attributed to the plugging of the pores. In other word, copper oxides deposited on the walls and/or in the mouth of the smaller pores, leading to the decrease in the BET area.

Table-1: Physical property of supported Cu catalysts.

Catalyst	BET Surface Area (m ² g ⁻¹)	Average Pore Diameter (nm)	Pore Volume (cm ³ g ⁻¹)
5Cu/γ-Al ₂ O ₃	287.3	10.3	0.7
5Cu/ZrO ₂	149.8	3.1	0.1
5Cu/SiO ₂	295.6	11.1	0.8
5Cu/HZSM-5	348.3	7.9	0.5

XRD was carried out to identify the phase structure of all four catalysts (Fig. 1). Clearly, Cu supported on ZrO₂ and SiO₂ was either completely X-ray amorphous in phase or too fine to be detected by XRD. It was found that no crystalline CuO was formed on the as-synthesized materials except 5Cu/SiO₂ (The catalysts are designated as xCu/support, in which x represents the quantity of the Cu metal (weight) loaded on per 100 gram of the support.), indicating that SiO₂ favored a better crystallization of CuO, which appeared to be amorphous on other supports.

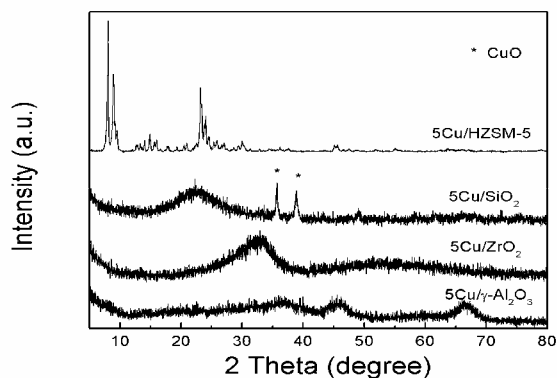


Fig. 1: XRD patterns of supported Cu catalysts.

Chemical State of Copper

It was well-known that the Binding Energy (BE) of CuO was about 933.3 eV for 2p_{3/2} and 953.5 eV for 2p_{1/2} [41]. Fig. 2 and 3 give the typical XPS spectra of supported Cu catalysts. It was found that in all samples, copper existed in the oxidation state of Cu²⁺, as evidenced by the Cu 2p_{3/2} peak at 933.6-934.3 eV with the shake-up satellite at 942.4-944.2 eV and the Cu 2p_{1/2} peak at 953.8-954.6 eV with the

shake-up satellite at 962.7-964.6 eV [42]. The spectra were fitted with two components for the Cu 2p_{3/2}, Cu 2p_{1/2} and two satellite peaks. The low energy peak could be generally attributed to Cu²⁺ located in octahedral sites, and the high binding energy peak might be ascribed to Cu²⁺ in tetrahedral sites [43]. The BE of Cu 2p_{3/2} decreased in the order of 5Cu/SiO₂ > 5Cu/HZSM-5 > 5Cu/ZrO₂ > 5Cu/γ-Al₂O₃, from 934.3 to 933.6 eV (Fig. 3). This result implied that the interaction between CuO and supports took place. According to other report [44], the BE of Cu 2p_{3/2} also appeared to correlate with the copper dispersion, i.e. a lower BE observed for the sample with a higher component dispersion and a higher BE for the sample containing bulk crystalline CuO. This was in accord with the XRD diffractograms (Fig. 1).

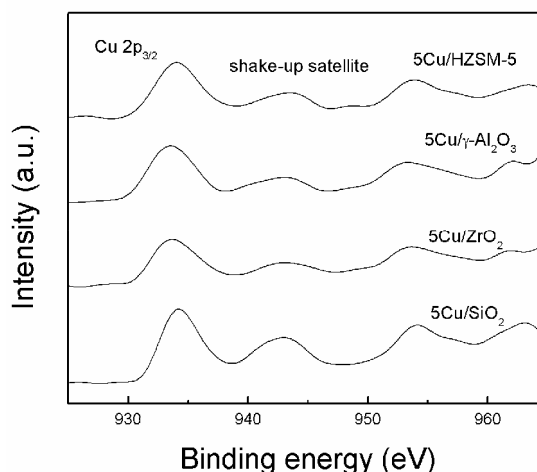


Fig. 2: XPS spectra of supported Cu catalysts.

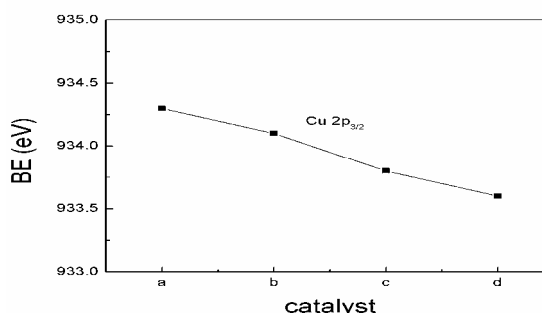


Fig. 3: Effect of the supports on the BE (eV) of Cu 2p_{3/2} for the supported Cu catalysts: a 5Cu/SiO₂; b 5Cu/HZSM-5; c 5Cu/ZrO₂; d 5Cu/γ-Al₂O₃.

Surface Acidity

Pyridine FT-IR was used for determining Lewis and Brønsted acid sites of the catalysts (see Fig. 4). In general, the bands at 1545 and 1640 cm^{-1} could be assigned to Brønsted acid sites [45]. Similarly, the bands at 1455 and 1607 cm^{-1} could be associated with Lewis acid sites, and the band around 1495 cm^{-1} was normally attributed to a combination band associated with both Brønsted and Lewis acid sites. Obviously, the pyridine FT-IR spectrums for both 5Cu/ZrO₂ and 5Cu/ γ -Al₂O₃ only showed bands associated with Lewis sites (at 1455 and 1607 cm^{-1}), but the co-existence of Brønsted sites (at 1545 and 1640 cm^{-1}) and Lewis sites (at 1455 and 1607 cm^{-1}) were evident for 5Cu/HZSM-5 in addition to the combination band at 1495 cm^{-1} . No Brønsted sites or Lewis sites was observed on 5Cu/SiO₂. These observations were in agreement with those reported in the literatures [46-49].

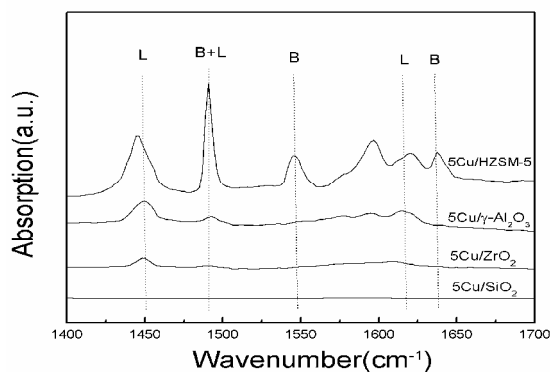


Fig. 4: FT-IR spectra of pyridine adsorbed on supported Cu catalysts.

NH₃-TPD for supported Cu catalysts was carried out for the acidity (Fig. 5). The total acid amount of catalysts decreased in the order of 5Cu/HZSM-5 \gg 5Cu/ γ -Al₂O₃ > 5Cu/ZrO₂ > 5Cu/SiO₂. The ammonia desorption spectra of 5Cu/HZSM-5 showed a desorption peak at 430 K with two shoulders ranged from 400 K to 700 K, and both 5Cu/ γ -Al₂O₃ and 5Cu/ZrO₂ exhibited a broad peak in the temperature range 350-530 K, but 5Cu/SiO₂ had a little desorption peak within all the temperature range. Furthermore, the high temperature peaks were observed for 5Cu/HZSM-5. These results indicated that there was no strong acid site on 5Cu/ZrO₂, 5Cu/ γ -Al₂O₃ and 5Cu/SiO₂ compared to 5Cu/HZSM-5. Obviously, their acidity was closely related to the nature of support.

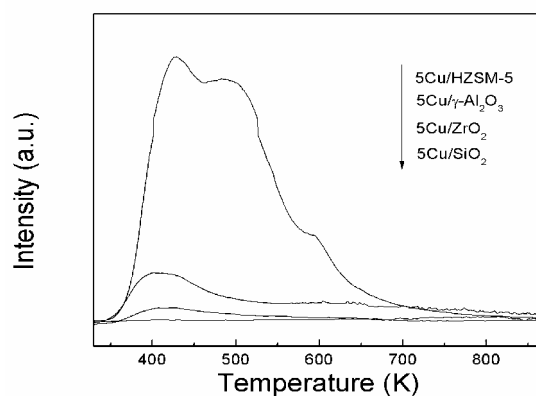


Fig. 5: NH₃-TPD profiles of supported Cu catalysts.

Reducibility

H₂-TPR illustrated that all the catalysts showed two well-defined peaks at 450-650 K (see Fig. 6). Several researchers [50-53] reported that the reduction of CuO followed a route of Cu²⁺ \rightarrow Cu⁺ \rightarrow Cu⁰, while others [54, 55] attributed the TPR peaks to the reduction of different CuO states. The hydrogen consumption indicated that the different peaks could not be assigned to the reduction of Cu²⁺ \rightarrow Cu⁺ \rightarrow Cu⁰. Therefore, the reduction processes were considered that the low temperature peak might be related to the reduction of well-dispersed CuO and the peak at high temperature should be corresponded to the reduction of large CuO particles for all supported Cu catalysts. Besides, the reduction temperatures increased along with 5Cu/ γ -Al₂O₃ < 5Cu/ZrO₂ < 5Cu/HZSM-5 < 5Cu/SiO₂, indicating that the nature of support had a strong effect on the reducibility of copper species.

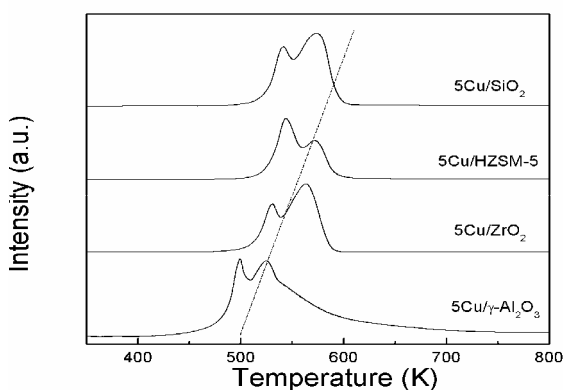


Fig. 6: TPR profiles of supported Cu catalysts.

Catalytic Performance

The hydrogenolysis of glycerol was carried out for the performance of supported Cu catalysts. The results in Table-2 indicated that 5Cu/HZSM-5 and 5Cu/SiO₂ had a low glycerol conversion (2.01% and 6.41%, respectively). A more pronounced support effect was observed over 5Cu/ZrO₂, for which the activity increased significantly to 37.79% in spite of its lower specific surface area, however, the selectivity to the desired product 1, 2-PD dropped significantly to 49.73%. The 5Cu/ γ -Al₂O₃ catalyst gave a glycerol conversion of 60.58%, showing both high activity and selectivity for the glycerol hydrogenolysis compared to others.

Table-2: The catalytic performance of glycerol hydrogenolysis over different supported Cu catalysts^a

Catalyst	Conversion (%)	Selectivity (%) ^b				
		1,2-PD	1-PO	EG	EtOH	MeOH
5Cu/ γ -Al ₂ O ₃	60.58	85.20	0.97	8.75	0.42	1.82
5Cu/ZrO ₂	37.79	49.73	41.56	6.21	0.31	1.42
5Cu/SiO ₂	6.41	80.39	-	4.13	8.23	0.45
5Cu/HZSM-5	2.01	65.83	-	1.87	20.68	5.32

^a Reaction conditions: 10 wt% glycerol aqueous solution; H₂ pressure: 6 MPa; catalyst weight: 4 g; reaction temperature: 513 K; LHSV: 0.9 h⁻¹
^b 1,2-PD = 1,2-propanediol; 1-PO = 1-propanol; EG = ethylene glycol; EtOH = ethanol; MeOH = methanol

It was believed that the pathway of glycerol hydrogenolysis involved a dehydration step on acidic sites followed by hydrogenation on metal sites [3, 13, 16, 18, 33, and 37]. However, an unexpected lower activity was observed from the most acidic 5Cu/HZSM-5, which was consistent with the result of Guo *et al.* [56]. They considered that acrolein instead of acetol was the preferred dehydration product on zeolites. In our opinion, this might be caused by coking due to the strong acidity of such a catalyst [57, 58], which encapsulated the active sites and then deactivated the catalyst. For 5Cu/SiO₂, the lower activity might be due to the lowest acidity and the large CuO particles, which led to a lower reduction of the copper oxides. As a result, the catalysts with the moderate acidity would be favorable for hydrogenolysis of glycerol. That was why 5Cu/ γ -Al₂O₃, which possessed an appropriate acidity, showed a better ability to activate the glycerol to form intermediates and then facilitated the formation of 1, 2-PD. Furthermore, it could also prevent the formed 1, 2-PD from consecutive hydrogenolysis to propanols.

The Cu/ γ -Al₂O₃ catalysts with different amounts of Cu were investigated to optimize the catalysts' composition for the glycerol hydrogenolysis. Table-3 presented the performance of those

catalysts at the condition of 513 K and 6 MPa. It could be observed that the glycerol conversion was as low as 3.68% over γ -Al₂O₃ without the formation of 1, 2-PD. The activity was greatly enhanced with 5% Cu incorporated into the catalyst system, and the conversion of glycerol increased to 60.58% with the 1, 2-PD selectivity of 85.20%. These results were similar with the reported literatures [30, 33], which confirmed that catalytic hydrogenolysis of glycerol should be performed over a bi-functional catalyst. Besides, the glycerol conversion reached a maximum for 20Cu/ γ -Al₂O₃. It was noted that the selectivity toward 1, 2-PD was almost constant irrespective of Cu loadings, suggesting that only a certain amount of Cu would be sufficient for hydrogenation to 1, 2-PD. Thus, the hydrogenolysis of glycerol needed a bi-functional catalyst.

Table-3: Effects of copper loading of Cu/ γ -Al₂O₃^a

Catalyst	Conversion (%)	Selectivity (%) ^b				
		1,2-PD	1-PO	EG	EtOH	MeOH
γ -Al ₂ O ₃	3.68	-	-	-	-	-
5Cu/ γ -Al ₂ O ₃	60.58	85.20	0.97	8.75	0.42	1.82
10Cu/ γ -Al ₂ O ₃	76.04	86.66	1.03	7.88	0.62	1.91
20Cu/ γ -Al ₂ O ₃	85.05	85.71	0.52	8.22	0.33	2.01
30Cu/ γ -Al ₂ O ₃	57.95	86.65	1.06	7.28	0.55	1.94
50Cu/ γ -Al ₂ O ₃	40.52	86.39	0.91	8.58	0.48	1.74

^a Reaction conditions: 10 wt% glycerol aqueous solution; H₂ pressure: 6 MPa; catalyst weight: 4 g; reaction temperature: 513 K; LHSV: 0.9 h⁻¹
^b 1,2-PD = 1,2-propanediol; 1-PO = 1-propanol; EG = ethylene glycol; EtOH = ethanol; MeOH = methanol

Furthermore, the temperature had a significant effect on the performance of 20Cu/ γ -Al₂O₃ (Table-4). As the temperature increased from 453 to 543 K, the glycerol conversion monotonically increased from 8.25% to 95.55%, but the 1, 2-PD selectivity declined from 87.64% to 35.65% with the increase of ethylene glycol and 1-propanol. This indicated that higher temperature would lead to the excessive hydrogenation of 1, 2-PD into other alcohols such as 1-propanol, ethylene glycol and other degradation products. Therefore, the high yield of 1, 2-PD required the optimal temperature which facilitated the conversion of those dehydrated intermediate and prevented the formation of 1, 2-PD from consecutive hydrogenolysis to 1-propanol.

Table-4: Effect of reaction temperature on the 20Cu/ γ -Al₂O₃ catalyst^a

Reaction Temperature (K)	Conversion (%)	Selectivity (%) ^b				
		1,2-PD	1-PO	EG	EtOH	MeOH
453	8.25	87.64	-	-	-	-
483	31.15	86.04	1.07	-	0.42	-
513	85.05	85.71	0.52	8.22	0.33	2.01
543	95.55	35.65	40.46	10.28	2.65	3.96

^a Reaction conditions: 20Cu/ γ -Al₂O₃, 10 wt% glycerol aqueous solution; H₂ pressure: 6 MPa; catalyst weight: 4 g; LHSV: 0.9 h⁻¹
^b 1,2-PD = 1,2-propanediol; 1-PO = 1-propanol; EG = ethylene glycol; EtOH=ethanol; MeOH = methanol

Fig. 7 showed the effect of pressure on the conversion and selectivity. The conversion of glycerol and the selectivity to 1, 2-PD over 20Cu/ γ -

Al₂O₃ increased with the rise of hydrogen pressures from 6 to 9 MPa. However, the increment showed a small change within the pressure range in the present work. Furthermore, the glycerol concentration also influenced the conversion of glycerol and the selectivity of 1, 2-PD (Fig. 8). The decrease of the conversion showed a near linear relation with the glycerol concentration increased from 10 to 50%. However, the selectivity toward 1, 2-PD remained almost constant in this case.

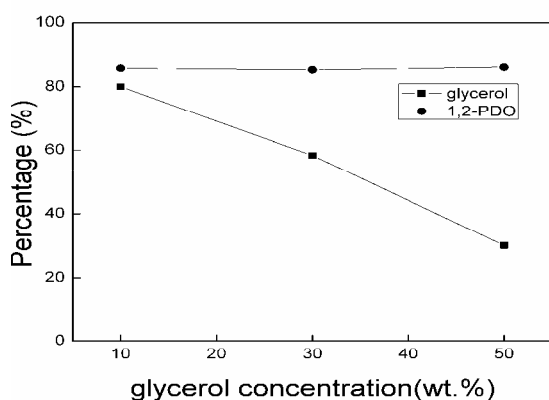


Fig. 7: Effect of reaction pressure on the 20Cu/γ-Al₂O₃ catalyst at 513 K and LHSV: 0.9 h⁻¹.

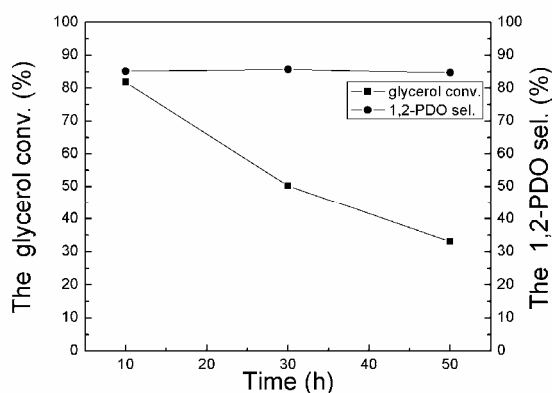


Fig. 8: Effect of glycerol concentration on the 20Cu/γ-Al₂O₃ catalyst at 513 K, 6MPa and LHSV: 0.9 h⁻¹.

Experimental

Catalyst Preparation

Supported Cu catalysts were prepared by means of incipient wetness impregnation method similar to that described in the literature [40]. Aqueous solutions containing specified amounts of Cu(NO₃)₂·3H₂O were prepared and impregnated onto different supports. The supports used in this study

included γ-Al₂O₃ (selfmade, 292.7 m²g⁻¹), ZrO₂ (selfmade, 165.8 m²g⁻¹), SiO₂ (Qingdao Haiyang Co., Ltd., China, 334.7 m²g⁻¹), and HZSM-5 zeolite (Nankai University Catalyst Co., Ltd., China, SiO₂/Al₂O₃ = 52, 367.9 m²g⁻¹). The supports were crushed and sieved to the powder form of 20–40 mesh. After impregnation, the catalysts were dried at 393 K overnight and calcined at 623 K for 5 h in air, and finally reduced at 573 K for 3 h in a H₂ stream (40 ml/min) before reaction.

Catalyst Characterization

To understand the performance of the catalysts, the different techniques were used to measure the catalysts properties such as pore size, surface area, structure, acidity and reducibility. The catalysts as-prepared were characterized using the follow techniques: N₂ adsorption–desorption, XRD, XPS, FT-IR, NH₃-TPD and TPR.

BET surface areas, pore volumes, and average pore diameters of the catalysts were determined by N₂ adsorption–desorption method at 77 K using a Micromeritics Tristar 3000 instrument. The samples were degassed under vacuum at 473 K for 12 h before the measurement. The average pore diameters were calculated according to BJH method.

XRD patterns of the catalysts were recorded on a Rigaku Miniflex (M/s. Rigaku Corporation, Japan) X-ray diffractometer using Ni filtered Cu Kα radiation (k = 1.5406 Å) with a scan speed of 2° Min⁻¹ and a scan range of 5–90° at 30 kV and 15 mA.

XPS analyses were carried out with a Perkin-Elmer PHI-5400 spectrometer, using a monochromatic Mg Kα radiation (1253.6 eV). Samples were compressed in small cup under the pressure of 5 kg/cm² for 30 s and supported on a holding ceramic carousel. The positive charge, developed on the samples due to the photoejection process was compensated by a charge neutralizer (Low energy electron and Low energy ion beam). The residual pressure in the spectrometer chamber was 5 × 10⁻⁷ Pa during data acquisition. The analyzed area of the sample was 100 μm and the Energy regions of the photoelectrons were scanned at a pass energy of 29.35 eV. The resolution was 0.68 eV. Binding energy (BE) reference was taken at the C1s peak of the carbon contaminating the surface of the samples at a value of 284.6 eV. The data was treated on Phi Multipack Program, Gaussian/Lorentzian = 80%.

FT-IR measurements were made in the hydroxyl group and pyridine regions using Nicolet Nexus 470 Infrared spectrophotometer. Prior to each IR experiment, compressed sample (in form of a self-supporting wafer, ca. 6 mg/cm²) placed in the IR cell (with CaF₂ windows) was first subjected to evacuation treatment at 573 K for 3 h, followed by saturated adsorption of pyridine at room temperature (298 K) for 1 h and subsequent removal of physisorbed pyridine under vacuum at 423 K for 2 h, the sample was then allowed to cool to room temperature and the spectra were recorded.

NH₃-TPD analyses were conducted in a self-made apparatus. The catalyst sample (200 mg) was first purged by Ar for 2 h at 473 K, then cooled down to room temperature and NH₃ adsorption was carried out by passing a 30% NH₃/Ar mixture for 1 h. Afterwards, the residual NH₃ was eliminated by flowing dry Ar at the same temperature, the temperature was then raised to 873 K at a heating rate of 10 K/min and the desorption of NH₃ were recorded by a Balzers Mass Spectrometry (m/z=16 was used to avoid the influence of water).

TPR analyses were performed on a conventional apparatus with a thermal conductivity detector (TCD). 50 mg samples were loaded in a quartz tube and purged with Ar at 423 K for 60 min, and then cooled to 333 K. Reduction was carried out from 333 up to 1073 K (10 K/min) in a 10% H₂/Ar mixture with a flow rate of 30 ml/min.

Catalytic Test

The hydrogenolysis of glycerol in liquid phase was carried out in a fixed-bed reactor (stainless steel tube, length 800 mm and i.d. 20 mm) with a back pressure valve to control the reaction pressure. Prior to reaction, the catalysts were reduced in the hydrogen with a flow rate of 40 mL/min at 573 K for 5 h. The products were analyzed by HPLC (Schimadu LC-2010Avp, Kromasil-C18, 5 μ, 4.6 mm×250 mm stainless steel column). The reaction was usually conducted for 8 h and the condensed products during the first hour of the reaction were abandoned due to poor material balance. Glycerol conversion and production selectivity were defined as following:

$$\text{Conversion of glycerol (\%)} = \frac{\text{Sum of C mol of all liquid products}}{\text{Added glycerol before reaction}} \times 100\%$$

$$\text{Selectivity (\%)} = \frac{\text{C mol of each liquid product}}{\text{Sum of C mol of all liquid products}} \times 100\%$$

Conclusions

Supported Cu catalysts were investigated for the glycerol hydrogenolysis. It was found that the supports strongly influenced the catalytic performance via their properties. XRD, XPS and H₂-TPR characterization indicated that the interaction between CuO and supports took place, and the supports had strong effect on the reducibility of CuO. On the basis of the reaction and characterization results, it could be deduced that the catalyst with a moderate acidity would be favorable for the glycerol hydrogenolysis. It was also concluded that the hydrogenolysis of glycerol should be performed over a bi-functional (acid/metal) catalyst. Among those supports, therefore, γ-Al₂O₃ supported Cu catalyst showed higher activity and selectivity to 1, 2-PD with the optimal copper loading of 20%. In addition, the conversion of glycerol and the selectivity to 1, 2-PD also depended on the reaction temperature, pressure and glycerol concentration. The optimum performance over 20Cu/γ-Al₂O₃ was observed at 513K, 6MPa H₂ and LHSV of 0.9 h⁻¹ in 10 wt% glycerol aqueous solutions.

References

1. S. Y. Zhang, M. A. Dube, D. D. McLean and M. Kates, *Bioresource Technology*, **89**, 1 (2003).
2. T. Miyazawa, S. Koso, K. Kunimori and K. Tomishige, *Applied Catalysis A: General*, **318**, 244 (2007).
3. I. Furikado, T. Miyazawa, S. Koso, A. Shimao, K. Kunimori and K. Tomishige, *Green Chemistry*, **9**, 582 (2007).
4. E. P. Maris and R. J. Davis, *Journal of Catalysis*, **249**, 328 (2007).
5. M. Watanabe, T. Iida, Y. Aizawa, T. M. Alda and H. Inomata, *Bioresource Technology*, **98**, 1285 (2007).
6. E. Tsukuda, S. Sato, R. Takahashi and T. Sodesawa, *Catalysis Communication*, **8**, 1349 (2007).
7. H. Atia, U. Armbruster and A. Martin, *Journal of Catalysis*, **258**, 71 (2008).
8. S. H. Chai, H. P. Wang, Y. Liang and B. Q. Xu, *Green Chemistry*, **9**, 1130 (2007).
9. T. Hirai, N. Ikenaga, T. Miyake and T. Suzuki, *Energy Fuel*, **19**, 1761 (2005).
10. N. J. Luo, X. W. Fu, F. H. Cao, T. C. Xiao and P. P. Edwards, *Fuel*, **87**, 3483 (2008).
11. A. J. Byrd, K. K. Pant and R. B. Gupta, *Fuel*, **87**, 2956 (2008).
12. K. Lehnert and P. Claus, *Catalysis*

- Communication*, **9**, 2543 (2008).
13. J. Chaminand, L. A. Djakovitch, P. Gallezot, P. Marion, C. Pinel and C. Rosier, *Green Chemistry*, **6**, 359 (2004).
 14. D. G. Lahr and B. H. Shanks, *Journal of Catalysis*, **232**, 386 (2005).
 15. A. Perosa and P. Tundo, *Industrial and Engineering Chemistry Research*, **44**, 8535 (2005).
 16. M. A. Dasari, P. P. Kiatsimkul, W. R. Sutterlin and G. J. Suppes, *Applied Catalysis A: General*, **281**, 225 (2005).
 17. Y. Kusunoki, T. Miyazawa, K. Kunimori and K. Tomishige, *Catalysis Communication*, **6**, 645 (2005).
 18. T. Miyazawa, Y. Kusunoki, K. Kunimori and K. Tomishige, *Journal of Catalysis*, **240**, 213 (2006).
 19. T. Miyazawa, S. Koso, K. Kunimori and K. Tomishige, *Applied Catalysis A: General*, **318**, 244 (2007).
 20. T. Miyazawa, S. Koso, K. Kunimori and K. Tomishige, *Applied Catalysis A: General*, **329**, 30 (2007).
 21. J. Feng, J. Wang, Y. Zhou, H. Fu, H. Chen and X. Li, *Chemistry Letters*, **36**, 1274 (2007).
 22. J. Feng, H. Fu, J. Wang, R. Li, H. Chen and X. Li, *Catalysis Communication*, **9**, 1458 (2008).
 23. A. Alhanash, E. F. Kozhevnikova and I. V. Kozhevnikov, *Catalysis Letters*, **120**, 307 (2008).
 24. L. Ma, D. He and Z. Li, *Catalysis Communication*, **9**, 2489 (2008).
 25. M. Balaraju, V. Rekha, P. S. S. Prasad, B. L. A. P. Devi, R. B. N. Prasad and N. Lingaiah, *Applied Catalysis A: General*, **354**, 82 (2009).
 26. A. Brandner, K. Lehnert, A. Bienholz, M. Lucas and P. Claus, *Topics in Catalysis*, **52**, 278 (2009).
 27. T. Kurosaka, H. Maruyama, I. Naribayashi and Y. Sasaki, *Catalysis Communication*, **9**, 1360 (2008).
 28. Z. Yuan, P. Wu, J. Gao, X. Lu, Z. Hou and X. Zheng, *Catalysis Letters*, **130**, 261 (2009).
 29. M. Balaraju, V. Rekha, P. S. S. Prasad, R. B. N. Prasad and N. Lingaiah, *Catalysis Letters*, **126**, 119 (2008).
 30. L. C. Meher, R. Gopinath, S. N. Naik and A. K. Dalai, *Industrial and Engineering Chemistry Research*, **48**, 1840 (2009).
 31. C. Liang, Z. Ma, L. Ding and J. Qiu, *Catalysis Letters*, **130**, 169 (2009).
 32. L. Huang, Y. L. Zhu, H. Y. Zheng, G. Q. Ding and Y. W. Li, *Catalysis Letters*, **131**, 312 (2009).
 33. S. Wang and H. C. Liu, *Catalysis Letters*, **117**, 62 (2007).
 34. Z. Huang, F. Cui, H. Kang, J. Chen, X. Zhang and C. Xia, *Chemistry of Materials*, **20**, 5090 (2008).
 35. C. W. Chiu, A. Tekeei, W. R. Sutterlin, J. M. Ronco and G. J. Suppes, *Aiche Journal*, **54**, 2456 (2008).
 36. C. W. Chiu, A. Tekeei, J. M. Ronco, M. L. Banks and G. J. Suppes, *Industrial and Engineering Chemistry Research*, **47**, 6878 (2008).
 37. L. Huang, Y. L. Zhu, H. Y. Zheng, Y. W. Li and Z. Y. Zeng, *Journal of Chemical Technology and Biotechnology*, **83**, 1670 (2008).
 38. M. W. M. Tuck, Davy Process Technology Ltd. London W26LE, Great Britain, (CI. C07C29/132; C07C31/20), 31 Jan. 2008, GB Appl. 2008/012,244, 26 Jul. 2006; 20pp.
 39. S. Sato, M. Akiyama, K. Inui and M. Yokota, *Chemistry Letters*, **38**, 560 (2009).
 40. J. Zhou, Y. Zhang, X. Guo, A. Zhang and X. Fei, *Industrial and Engineering Chemistry Research*, **45**, 6236 (2006).
 41. R. P. Vasquez, *Surface Science Spectra*, **5**, 262 (1998).
 42. F. Raimondi, K. Geissler, J. Wambach and A. Wokaun, *Applied Surface Science*, **189**, 59 (2002).
 43. J. F. Moulder, W. F. Stickle, P. E. Sobol and K. D. Bomben, Handbook of X-ray Photoelectron Spectroscopy, in J. Chastain (Ed.), Perkin-Elmer Corporation Physical Electronics Division, Eden Prairie-Minnesota, p. 256 (1992).
 44. C. Z. Yao, L. C. Wang, Y. M. Liu, G. S. Wu, Y. Cao, W. L. Dai, H. Y. He and K. N. Fan, *Applied Catalysis A: General*, **297**, 151 (2006).
 45. F. Babou, G. Coudurier and J. C. Vedrine, *Journal of Catalysis*, **52**, 341 (1995).
 46. J. D. Adjaye, S. P. R. Katikaneni and N. N. Bakhshi, *Fuel Processing Technology*, **48**, 115 (1996).
 47. R. Anand, R. Maheshwari, K. U. Gore, S. S. Khaire and V. R. Chumbhale, *Applied Catalysis A: General*, **249**, 265 (2003).
 48. Y. V. Plyuto, I. Babich, L. Sharanda and A. Marco de Wit, *Journal of Molecular Thermochimica Acta*, **335**, 87 (1999).
 49. H. Dabbagh, M. Yalfani and B. Davis, *Journal of Molecular Catalysis A: Chemical*, **238**, 72 (2005).
 50. H. Oguchi, T. Nishiguchi, T. Matsumoto, H. Kanai, K. Utani, Y. Matsumura and S. Imamura, *Applied Catalysis A: General*, **281**, 69 (2005).
 51. E. D. Guerreiro, O. F. Gorriiz, J. B. Rivarola and L. A. Arrua, *Applied Catalysis A: General*, **165**,

- 259 (1997).
52. A. J. Marchi, J. L. G. Fierro, J. Santamaria and A. Monzon, *Applied Catalysis A: General*, **142**, 375 (1996).
53. K. V. R. Chary, K. K. Seela, G. V. Sagar and B. J. Sreedhar, *Journal of Physical Chemistry B*, **108**, 658 (2004).
54. P. A. Sermon, K. Rollins, P. N. Reyes, S. A. Lawrence, M. A. M. Luengo, and M. J. Davies, *Journal of the Chemical Society, Faraday Transactions 1*, **83**, 1347 (1987).
55. G. Fierro, M. L. Jacono, M. Inversi, P. Porta, F. Cioci and R. Lavecchia, *Applied Catalysis A: General*, **137**, 327 (1996).
56. L. Y. Guo, J. X. Zhou, J. B. Mao, X. W. Guo and S. G. Zhang, *Applied Catalysis A: General*, **367**, 93 (2009).
57. Y. Zhang, G. H. Xie, J. W. Liu, S. H. Yan and J. F. Shen, *Natural Gas Chemical Industry*, **33**, 24 (2008).
58. E. Tsukuda, S. Sato, R. Takahashi, T. Sodesawa, *Catalysis Communication*, **8**, 1349 (2007).